

Studies of Physical Aging and Molecular Motion by Azochromophoric Labels Attached to the Main Chains of Amorphous Polymers

L. Lamarre and C. S. P. Sung*

Department of Materials Science and Engineering, Massachusetts Institute of Technology, Cambridge, Massachusetts 02139. Received November 15, 1982

ABSTRACT: Azochromophores are used as molecular labels in the main chains of polyurethane to study molecular motion and physical aging in amorphous, single-phase matrices. Kinetics of both $\text{trans} \rightleftharpoons \text{cis}$ photoisomerization and $\text{cis} \rightarrow \text{trans}$ thermal isomerization are analyzed for dilute solutions as well as in the solid state covering the rubbery and glassy states. Photoisomerization in dilute solution occurs by a single-rate process with little temperature dependence in the range -10 to $+40$ °C. In solid films analogous photoisomerization seems to proceed by two separable processes, one as fast as in dilute solution and a slower one. The fractional amount of the fast process, α , increases slowly with temperature but shows a transition around T_g . With increasing aging time, α decreases in the glassy state with approximately the same time scale as enthalpy relaxation. At lower temperature, α decreases more slowly with aging time, a trend consistent with enthalpy or volume relaxation. When the film is plasticized or stretched at a temperature just below T_g , α increases. These trends suggest that α is a sensitive characteristic of free volumes or holes present in the solid matrices under investigation. A plausible way to interpret these results is to assume that α is related to the fraction of free volumes which are greater than a critical size or to the amount of the high segmental mobility associated with less dense regions in solids. Thus, the photochromic labels can provide some quantitative information on the structural changes occurring in amorphous polymeric solids. Thermal isomerization exhibits first-order kinetics either in dilute solution or in the rubbery state with an activation of about 18 kcal/mol. Deviation from first-order kinetics is observed in glassy films. The effect of physical aging on thermal isomerization seems rather small, probably due to the slower time scale of thermal isomerization.

Introduction

This work concerns the molecular characterization of physical aging and molecular motion in polymeric solids. Physical aging¹ refers to the process when quenched polymeric glasses slowly reach an equilibrium state from a nonequilibrium state with concurrent loss of volume and enthalpy. As well as showing densification, the glassy polymers become more brittle as a consequence of physical aging.² This phenomenon is usually studied as a function of isothermal annealing time below T_g . Research into physical aging is directed at both experimental and theoretical³ studies. Among the experimental techniques, volume,⁴ enthalpy⁵ relaxations, or mechanical property^{2,6} measurements are often made. In this study, we describe for the first time the characterization of physical aging at the molecular level, using a photochromic labeling technique. As pointed out by Williams and Daly⁷ in a recent review, the dominant factor in the photochemistry of labels in polymeric solids is the local free volume in the vicinity of the label, because their signals are strongly dependent on the rotational mobility of the label in the matrix. This effect has been found to be true also in ESR spin labels.⁸ This sensitivity of the label to the local free volume can be utilized to probe the amorphous structure. Since physical aging reduces free volume, it is reasonable to expect that the behavior of a photochemical label will be affected by it. It is essential that the label be truly molecularly dispersed in the matrix and not in any way aggregated. Thus, molecular probe studies in which labels are merely dispersed in the matrix may be less definitive than studies of labels chemically bonded to the matrix. Recent studies by Law and Loutfy⁹ indicate that molecular dispersion of dyes in polymers is only achieved at very low concentrations (<0.03 M). Furthermore, in molecular labeling studies, labels can be selectively attached to the side chain, main chain, or chain ends of the polymer. Such selective-site labeling would hopefully allow one to identify motions associated with the specific location of the polymer chain and will, therefore, be more informative than molecular probe studies.

In this study, we employ a photochromic labeling technique using an azobenzene derivative. The method is to follow the photochemical $\text{trans} \rightleftharpoons \text{cis}$ isomerization of the azochromophore by UV-vis spectroscopy and extracting kinetic parameters for evaluation as a function of temperature and physical aging time. The photochemistry of azobenzene has been extensively investigated.¹⁰ In earlier work, Paik and Morawetz¹¹ and Eisenbach¹² utilized polymers having azochromophores attached to the side chains. They found that the quantum yield of the photochemical isomerization was reduced in glassy films by about an order of magnitude as compared to the dilute solution. The thermal $\text{cis} \rightarrow \text{trans}$ isomerization in the glassy films deviated from the first-order kinetics with a fraction of the azo groups relaxing with an anomalously fast rate. When the azo label was incorporated into the main chain of the polymer, it was found that photoisomerization was greatly reduced in the glassy state.^{11,13} The effects of physical aging on isomerization behavior were not studied, as these polymers had high T_g values.

In this work, we incorporated azochromophores into the main chain of amorphous, single-phase polyurethanes with T_g in the range 8–45 °C. This enabled us to study the isomerization behavior in both the glassy and the rubbery states.

We found that the photoisomerization of azo labels in the main chains of a polymeric glass is affected greatly by physical aging and seems to occur by at least two separable processes, one as rapid as in dilute solution and one slow process.¹⁴ Therefore, as an approximation, it becomes possible to estimate the fraction of azochromophores in liquid-like environments in the glassy state by using a simple analyses based on a two-rate process. This fraction decreases with increasing physical aging and with decreasing temperature. This behavior can be analyzed in terms of free volume theory.

Other factors such as plasticization, tensile deformation¹⁵ in the glassy state, or hydrostatic pressure¹⁶ are expected to change the free volume (or holes) and its distribution. In order to demonstrate that such effects can also be

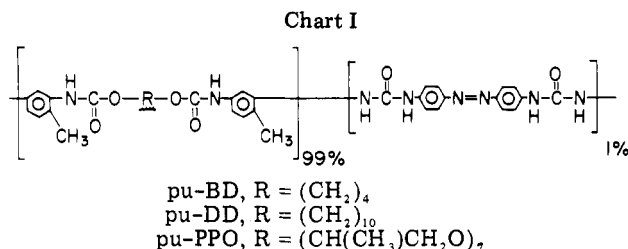


Table I
Characteristics of the Labeled Polymers

property	polymer		
	pu-PPO	pu-DD	pu-BD
λ_{\max}^a , nm	379	379	385
T_g^b , °C	8	15	45
density at 25 °C, ^c g/cm ³	1.135	1.139	1.224
η_{inh}^d	0.49	0.64	0.27

^a λ_{\max} corresponding to $\pi \rightarrow \pi^*$ transition of azo residues. ^b By differential scanning calorimetry. ^c Measured in a density gradient column. ^d Measured at 40 °C at a polymer concentration of 0.3 g/dL in DMF-LiBr (0.05 mol) solution except for pu-BD, measured in DMF solution.

sensitively monitored by our labeling techniques, we report a limited study of the effect of plasticization by residual solvent and of the tensile deformation in the glassy state.

The thermal cis \rightarrow trans isomerization is a much slower process than photoisomerization with an activation energy of about 20 kcal/mol. It is also of interest to see whether such slow motions may be affected by physical aging.

Experimental Section

Syntheses of Labeled Polymers. Three polymers were prepared by a solution polymerization method in dry glassware under an inert nitrogen atmosphere. Toluene 2,4-diisocyanate (2,4-TDI) from Aldrich Chemical Co. was vacuum distilled before use. A solution of 4,4'-diaminoazobenzene (0.001 mmol) in 10 mL of dimethyl sulfoxide (Matheson Coleman and Bell, ACS Reagent Grade) was added to a solution of purified 2,4-TDI (0.1 mL) in 70 mL of dimethyl sulfoxide and allowed to react for 15 min at 100 °C. This was followed by the injection of the specific diol (0.099 mol), and the polymerization was allowed to proceed for 30 min at 100 °C. The NCO/(OH + NH₂) ratio was carefully kept to 1.0 to ensure the linear-chain structure of the polymer. The polymers were precipitated, washed, and vacuum-dried at 50 °C for 10 days. Chart I shows the chemical structure of the three labeled polyurethanes. The three polyurethanes are designated as pu-PPO, pu-DD, or pu-BD depending on the diol used in the composition.

Characterization of Labeled Polymers. Table I summarizes the physical characteristics of the labeled polymers. The glass transition temperature was measured by using a Perkin-Elmer DSC-II at a heating rate of 20 °C/min, by taking the midpoint in the change of the slope in the DSC scan. For our labeled pu-BD and pu-DD, the observed glass transition temperatures are very similar to the reported DSC values for unlabeled polyurethanes.¹⁷ This result is reasonable since the incorporation of a small amount of azochromophore (<0.01 mol %) in these single-phase, amorphous polymer matrices is not expected to raise T_g significantly.

Isomerization Studies. Thin polymer films, about 10 μm in thickness, were cast directly onto a quartz plate (1 in. \times 1 in.) from filtered 2.5% solutions of the polymer in DMF and dried in a vacuum oven at about 20 °C above its T_g for several days to remove the solvent. The optical density at λ_{\max} for the azo residue was in the range 0.7–1.0. Quenching of the samples was done from 10 to 12 °C above T_g to the specific glassy temperature, with the same cooling rate of 160 °C/min in the DSC for all samples. The cooling rate in the isomerization kinetic studies was slower and thus, the quenched state in the kinetic studies

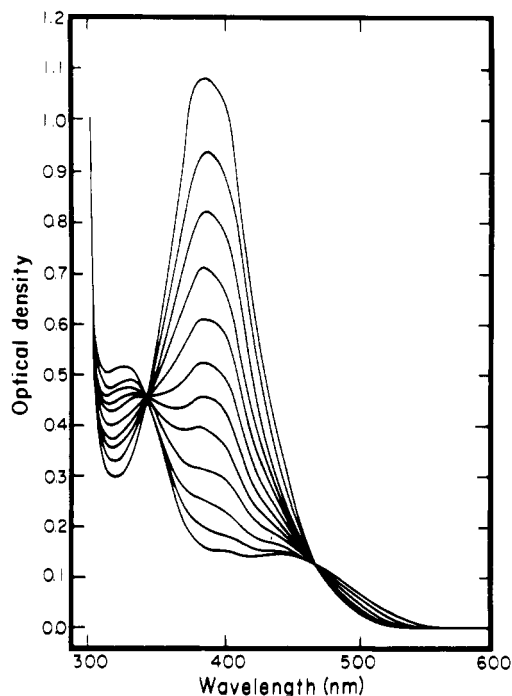


Figure 1. UV-vis absorption spectra of azobenzene residues in pu-BD in dilute DMF solution as a function of irradiation time (top curve before irradiation and bottom curve at the photo-stationary state, at light intensity of 1 mW/cm²; the intermediate curves are obtained at an intermediate radiation interval).

actually corresponds to about 5–8 min of physical aging. Photoisomerization kinetics were always started with all-trans isomers by heating the sample to convert any cis (isomer) to trans isomers. The irradiation intensity (I_0) was determined to be 5.5 mW/cm² unless otherwise noted. Kinetic studies were carried out in a Cary 14 spectrophotometer, which was modified so that samples could be alternately irradiated by a 450-W xenon Osram lamp and analyzed for absorbance changes in a direction perpendicular to the irradiation direction. Before monitoring thermal cis \rightarrow trans isomerization, we carried out photochemical trans \rightarrow cis isomerization to reach a photostationary state in case of dilute solution or at least 50% conversion in case of films. The physical aging effect on the thermal isomerization was studied in the following manner: First, photoisomerization was carried out in the rubbery state, and the sample was quenched to the glassy temperature, followed by isothermal aging with the irradiation continuing on the sample. The thermal dark reaction was then followed.

Results and Discussion

(a) Photoisomerization in Dilute Solution. The azo moiety in the polymer shows a distinctive UV-vis spectrum in the 300–600-nm range without overlap from the matrix polymer, as shown in Figure 1. The matrix polymer shows UV absorption below 300 nm. The top curve in Figure 1 corresponds to the spectrum before irradiation; therefore, all the azochromophores are in the trans state. The λ_{\max} at around 380 nm is due to the $\pi \rightarrow \pi^*$ transition. As the solution is irradiated, the absorption at λ_{\max} decreases while absorptions at 320 and 444 nm increase. The absorption at 320 nm corresponds to the $\pi \rightarrow \pi^*$ transition of the cis isomer while the peak at 444 nm is due to the $n \rightarrow \pi^*$ transition of both isomers. The $n \rightarrow \pi^*$ transition is stronger for the cis isomer; thus the intensity increases with irradiation. Two isosbestic points at 335 and 458 nm can be observed, indicating that only trans and cis isomers are present. The bottom curve in Figure 1 corresponds to about 95% cis isomer and 5% trans isomer at the photo-stationary state. In estimating the isomer composition, we resolved the spectra with three peaks and used the optical density at λ_{\max} for the $\pi \rightarrow \pi^*$ transition after

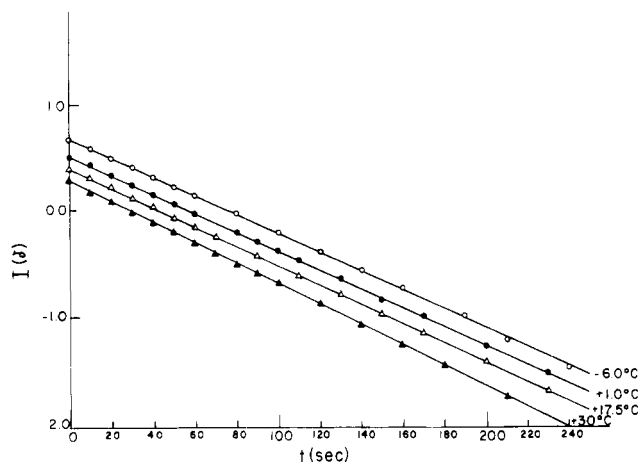


Figure 2. Kinetics of photochemical $\text{trans} \rightleftharpoons \text{cis}$ isomerization of azobenzene residues in pu-PPO in dilute DMF solution as a function of irradiation time (with light intensity of 1 mW/cm^2).

correction for the overlaps for the 320- and 444-nm peaks.

In dilute solutions, all three polymers show completely reversible photoisomerization behavior with a 95% cis content at the photostationary state.

The kinetics of photochemical $\text{trans} \rightleftharpoons \text{cis}$ isomerization have been followed by monitoring corrected optical densities at λ_{max} for the $\pi \rightarrow \pi^*$ transition and analyzed with eq 1, which is a good approximation of the solution of the reversible photochemical rate equation when the thermal isomerization is negligible.¹⁸

$$I(\delta) \simeq \left(1 + \frac{D_{\infty}}{2} + \frac{D_{\infty}^2}{12} \right) \ln \delta - \left(\frac{1}{2} + \frac{D_{\infty}}{6} \right) \delta + \frac{\delta^2}{24} = -At + \text{const} \quad (1)$$

where $\delta \equiv D_{\infty} - D$ and D_{∞} and D are optical densities at the photostationary state and at time t , respectively. The plots of $I(\delta)$ vs. t (irradiation time) were linear when azobenzene was studied in dilute solution. From the slopes (A), the quantum yield for $\text{trans} \rightarrow \text{cis}$ isomerization (ϕ_t) has been estimated since $A = I_0 \phi_t \epsilon_t / Y_{\infty}$, where I_0 is irradiation intensity, ϵ_t the molar extinction coefficient of the trans isomer, and Y_{∞} the fraction of cis isomer at the photostationary state. Zimmerman et al. obtained ϕ_t of about 0.12 and ϕ_c of about 0.40 for the $\pi \rightarrow \pi^*$ transition of azobenzene in dilute solution at 25°C .^{18a}

In Figure 2, $I(\delta)$ is plotted as a function of irradiation time for pu-PPO dilute solution at several temperatures. We also obtain linear $I(\delta)$ plots up to 90% conversion;¹⁹ the slopes are almost independent of temperature in this range (from -10 to $+40^\circ\text{C}$). For other polymers, the slopes of $I(\delta)$ plots were also independent of temperature with similar A values. Thus, results indicate that in dilute solution, the ability of the azo moiety to isomerize photochemically is not strongly influenced by the composition of the polymer chain, since the choice of a particular diol used for the polymer does not make much difference to the A values. This result is not surprising in view of the much faster time scale of photoisomerization in comparison to the motions of the polymer chain as demonstrated recently by Irie and Schnabel.²⁰ By using flash photolysis techniques, they reported that the $\text{cis} \rightarrow \text{trans}$ photoisomerization of the azobenzene moiety in an aromatic polyamide in solution occurs to about 90% during a 20-ns flash, with the remaining 10% complete within 100 ns after the flash. They also measured the relaxation time due to the conformational change of the total molecule in dilute solution following photoisomerization, using time-resolved light scattering measurement, and found it to be about 1

ms, much slower than the photochemical reaction.

From the experimentally determined values of I_0 , ϵ_t , and Y_{∞} , we obtained approximate values of ϕ_t and ϕ_c to be about 0.18 and 0.38, respectively, at the $\pi \rightarrow \pi^*$ transition of the azochromophore. In pu-PPO in dilute solution, our ϕ_t is somewhat higher than Zimmerman's value but ϕ_c is close to their value. The error in our measurements may be in part due to the fact that we do not use monochromatic light. Since the primary objective of our work is the comparison of the photoisomerization behavior of azo labels in solution with that occurring in the solid state, we preferred to use the slope of the $I(\delta)$ vs. time plot as characteristic of the behavior rather than as the absolute quantum yield. Whenever such comparison was made, it was with the same light intensity. Under such conditions, the slope, A , can be considered as a relative quantum yield or as a relative measure of the rate of photoisomerization toward equilibrium. It is useful to point out that such relative rates of photoisomerization toward the photostationary state reflected in the slope should not be confused with the rate constant of $k_{t \rightarrow c}$, which can be only obtained by knowledge of quantum yields and the excited-state lifetime. However, the exact mechanism (singlet vs. triplet) of photoisomerization of azobenzene is still controversial,¹⁰ which makes it difficult to measure the involved excited lifetime. Thus, no attempt has been made to measure $k_{t \rightarrow c}$ in this study.

(b) Photoisomerization in the Solid Films. In contrast to the behavior in dilute solution, the photochemical behavior in the solid films is nonlinear, which implies variations in the quantum yield ϕ_t . There is a fast process followed by a much slower process, approaching a photostationary-state composition similar to that in solution. In Figure 3, for convenience, $I'(\delta)$ is plotted vs. time, where $I'(\delta)$ is $I(\delta)$ minus the intercept at $t = 0$, where Y_{∞} is assumed to be the same as in solution. This curvature in the kinetic plot is present both in the rubbery state (Figure 3, top) and in the quenched glassy state (Figure 3, bottom). One may also note from Figure 3 that the slower process is only slightly dependent on the temperature of the matrix. A similar behavior is observed for all three polymers. Attempts to fit the initial portion of the curve with a distribution function appeared too laborious and complex, though such an approach can lead to better characterization of the process. In a simpler approach, we fitted empirically the initial portion of the curve (up to 400 s of irradiation time) by the sum of two processes:

$$e^{-I'(\delta)} = \alpha e^{-A_1 t} + (1 - \alpha) e^{-A_2 t} \quad (2)$$

where A_1 characterizes the fast process, A_2 characterizes the slow process, and α is the fraction characterized by the fast process. When A_2 was assumed to be $2 \times 10^{-4} \text{ s}^{-1}$ from the linear slopes of the slower process, α and A_1 can be estimated graphically. From the intercept ($\ln x_0$), α can be obtained since $\alpha = 1 - 1/x_0$. The slope of the plot of $\ln(x - y)$ vs. time gives A_1 , where $\ln x$ is a point on the extrapolated linear line and $\ln y$ is the corresponding point on the experimental curve. A value for A_1 of about $2 \times 10^{-2} \text{ s}^{-1}$ was obtained for all three polymers when I_0 was 5.5 mW/cm^2 , and this is about 100 times greater than A_2 . It is similar to the slope observed in dilute solution, when the same irradiation intensity was used. Therefore, the fraction of the fast rate (α) alone can characterize the photochemical kinetics occurring in the solid state. Figure 4 relates α to the temperature interval from T_g for pu-PPO and pu-BD polymers. The following can be observed from Figure 4. (1) While α is unity in dilute solution, α in the rubbery state also tends toward unity. (2) In the quenched glassy state, especially for pu-PPO, α is significantly larger

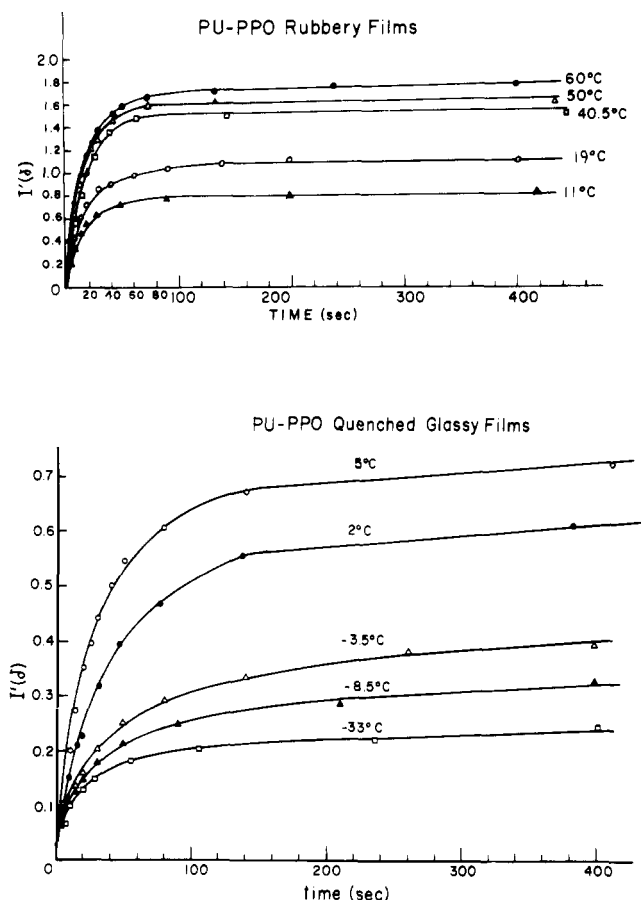


Figure 3. Kinetics of photochemical $\text{trans} \rightleftharpoons \text{cis}$ isomerization of azobenzene residues in pu-PPO solid films: (top) rubbery films; (bottom) quenched glassy films (with light intensity of 5.5 mW/cm^2). Here, $I'(\delta)$ is plotted rather than $I(\delta)$, where $I'(\delta)$ is $I(\delta)$ minus the intercept at $t = 0$.

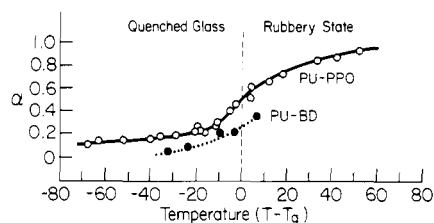


Figure 4. Plot of α (fraction which characterizes fast, liquid-like process) as a function of the distance from T_g for pu-PPO and pu-BD.

than zero (about 0.1) even at a temperature 70 °C below its T_g . In general, α values for pu-BD seem smaller than for pu-PPO which shows T_g at 8 °C but a β transition probably due to the PPO (MW = 400) around -55 °C as observed by DSC. The generally high mobility in the pu-PPO matrix even at such a low temperature may be related to the β transition associated with PPO.

(c) Physical Aging Effect on Photoisomerization in Glassy Films. While the photochemical isomerization of azo labels in pu-PPO (e.g., at 25 °C) is not influenced by the annealing of the film in the rubbery state, it is found to be strongly influenced by physical aging (isothermal annealing) at a sub- T_g temperature. For example, when a pu-PPO film is quenched from the rubbery state to the glassy state (e.g., 10 °C below T_g), its photoisomerization proceeds along the upper curve of Figure 5. If the sample is aged at 10 °C below T_g in the dark prior to irradiation, photoisomerization becomes progressively more difficult, as shown by several lower curves in Figure 5. After 1-day

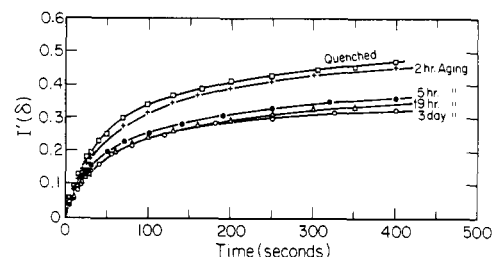


Figure 5. Kinetics of photochemical $\text{trans} \rightleftharpoons \text{cis}$ isomerization showing the effect of annealing in the glassy state (10 °C below T_g).

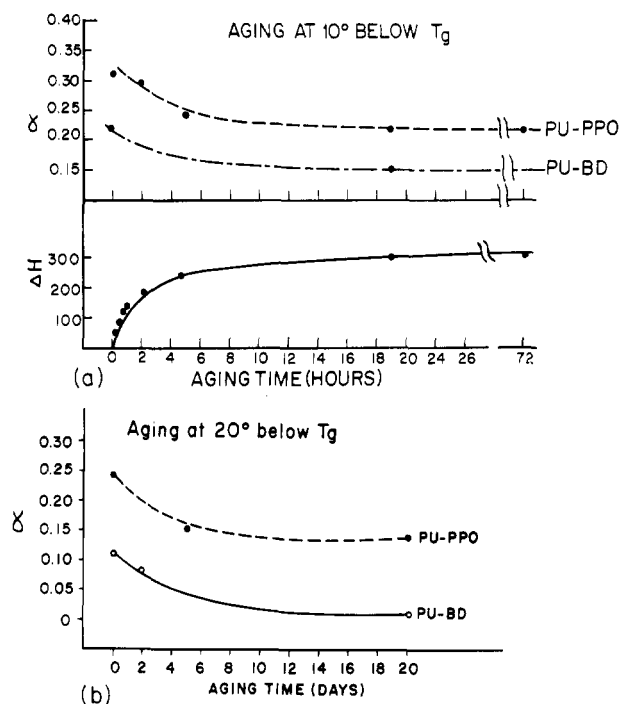


Figure 6. (a) Changes of α (fraction of fast process) and enthalpy relaxation (ΔH) as a function of isothermal (10 °C below T_g) aging time. (b) Changes of α as a function of isothermal aging time at 20 °C below T_g .

aging, the matrix appears to be near equilibrium because a further increase in aging time does not change the curve.

Possibly, with the decrease in total volume as the matrix ages, the decrease in the local volume surrounding the azo labels is manifested by the difficulty in its photoisomerization. In order to obtain more quantitative information on the kinetics, the curves in Figure 5 were analyzed by curve fitting again with two processes as discussed earlier. It was found that the same A_1 and A_2 values used for the rubbery or the quenched glassy states could be used to fit the curves. Therefore, the only variable during aging was α , the fraction which is characterized by the faster rate constant. Figure 6 shows the changes in α as a function of aging time at 10 °C below T_g . For quenched pu-PPO film α is about 0.31, which gradually decreases with aging time to about 0.22. For pu-BD, somewhat lower α values are observed.

In any molecular labeling study, a question can be raised as to whether the label monitors the overall matrix environment or a perturbed local environment in the vicinity of the label. Such a perturbation is expected to be more pronounced when the molar volume of the label far exceeds the activation volume²¹ ($\Delta V^* \approx 4k_1\Delta H_a$) of the matrix, where k_1 is the compressibility in the rubbery state and ΔH_a is an activation energy for the glass transition, as shown by Boyer and Kumler²² in ESR spin-probe studies.

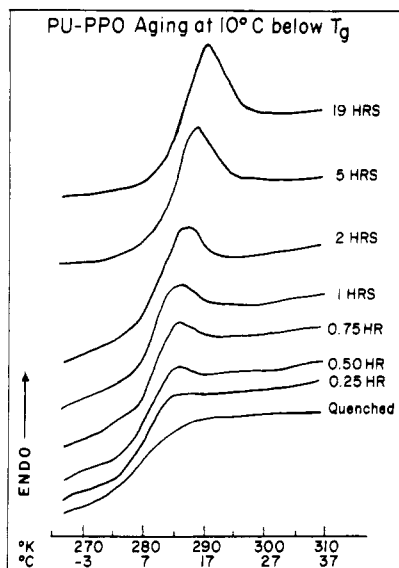


Figure 7. Enthalpy relaxation for pu-PPO at 10 °C below T_g as shown by DSC traces as a function of aging time.

They showed that $\log \Delta V^*$ increases linearly with T_g of the matrix. Higher mobility was observed well below T_g when the size of the probe is smaller than the activation volume of the matrix, while larger size probes do not become mobile until well above T_g . Only when the size of the label matches the activation volume of the matrix do the changes in the mobility of the ESR spin probe occur at the T_g of the matrix. Since the label in the pu-PPO matrix distinguishes the rubbery and glassy states in its time dependence, as illustrated in Figure 5, we feel that the molar volume of the azo label is reasonably close to the activation volume. As an additional check for the validity of the azo label to monitor the matrix, we followed enthalpy relaxations on the same matrix. Figure 7 shows representative DSC traces of the polymer which was aged at 10 °C below T_g . This type of DSC behavior, i.e., an endotherm increasing with aging time, is typical of glassy polymers as observed by Petrie and others.²³ The ΔH value, which corresponds to the graphic area measured from DSC traces by subtracting the DSC trace of the quenched sample,²³ can be used to follow the kinetics of aging as plotted in the lower part of Figure 6a. It is clear from Figure 6a that both α and enthalpy relaxation reach equilibrium after a similar time period (about 1 day). This rate compares well with the physical aging rate of polystyrene at 10 °C below its T_g as measured by Petrie⁶ by mechanical and enthalpy relaxation. When α and ΔH are plotted against $\log t$, ΔH shows a linear line while α is nonlinear. In fact, the α curve is similar to the general curve of the deviation $\delta \equiv (V - V_\infty)/V_\infty$ from the equilibrium volume.

At 20 °C below T_g , the photochemical kinetic profile can be analyzed by the same two processes, except that the physical aging is much slower as shown in Figure 6b of the plot of α as a function of physical aging. There is a progressive decrease in α for both pu-PPO and pu-BD over a period of 20 days, but even after 20 days, α for pu-PPO is greater than for pu-BD. In fact, for pu-BD, α approaches zero after 20 days or if the film is cast and slowly dried at 25 °C (20 °C below T_g).

(d) Effect of Residual Solvent and Tensile Deformation on Photoisomerization. As discussed in the preceding section, the trends observed in α values, i.e., decrease in α with decreasing temperature or increasing densification, suggest that α is a sensitive function of free volume present in amorphous glassy matrices under in-

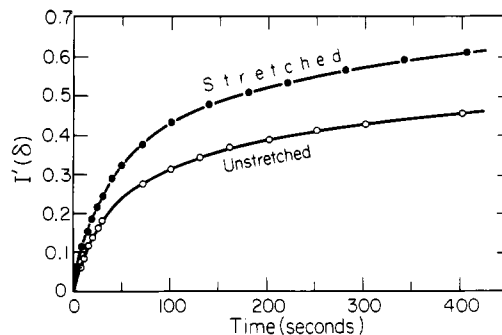


Figure 8. Effect of glassy deformation (uniaxial stretching) on the kinetics of photochemical isomerization for pu-PPO at -2 °C. (Upper curve is for a film stretched to ~20% at 0 °C and aged at -2 °C for 1 h; the lower curve is for undeformed film which was aged at -2 °C for 2 h.)

vestigation. Other factors such as plasticization, tensile deformation, or hydrostatic pressure are known to affect free volume in glassy matrices. In order to test if these effects also can be monitored sensitively by the photoisomerization behavior of the labels, we carried out some studies as described below.

When residual solvents are not completely removed from the cast film specimen (e.g., pu-DD), higher α values are observed in comparison to the extensively dried films. It is reasonable to expect that residual solvents act as plasticizer, providing more free volume and thus increasing α values.

It is well-known that tensile deformation in the glassy state increases free volume of the glassy polymer since the Poisson ratio in the glassy state is less than 0.5. For a small strain of uniaxial stretching, the volume change (ΔV) may be approximated to the strain (ϵ) and the Poisson ratio (ν) by the equation

$$\Delta V/V_0 \approx \epsilon(1 - 2\nu) \quad (3)$$

where V_0 is the original volume. Since ν is less than 0.5, it is seen in this equation that $\Delta V/V_0$ is always greater than zero. Such a volume change will become available as free volume,^{15b,24} and thus, the photochemical behavior of the azo label, is expected to be different after deformation. Quenched pu-PPO film was stretched at 0 °C uniaxially up to 20% of strain. At this temperature, the polymer is still somewhat viscoelastic rather than elastic. But at lower temperatures, crazing becomes an experimental problem. The upper curve in Figure 8 illustrates the photochemical behavior at 10 °C below T_g , showing a plot of $I'(\delta)$ vs. irradiation time for stretched pu-PPO film after 1-h aging. The analysis of the kinetic data by the same two processes shows that α for stretched film is 0.39 in comparison to 0.30 for unstretched film with similar aging time (corresponds to the lower curve in Figure 8). Thus, α increases significantly after stretching, reflecting an increase in free volume.

(e) Proposed Interpretation of Photoisomerization Results. In order to interpret these changes in α , we invoke the following critical size concept for photoisomerization: photoisomerization in the solid state can occur at a rate similar to that in dilute solution as long as the azo label has in its vicinity available free volume larger than a certain critical size. This type of critical size concept was found to account successfully for the viscosity dependence of $\text{trans} \rightleftharpoons \text{cis}$ photoisomerization of stilbene, some substituted stilbenes, and azobenzene in dilute solutions²⁵ and for the temperature dependence of the photoisomerization of azomethane in low molecular weight glasses.²⁶

It may be of interest to estimate the size of the critical volume necessary for the photoisomerization of azobenzene. Even though still controversial, the $\text{trans} \rightleftharpoons \text{cis}$ photoisomerization of azobenzene on $\pi \rightarrow \pi^*$ excitation is believed to proceed by a rotation mechanism, i.e., by twisting around the central $\text{N}=\text{N}$ double bond.^{10c} Since the end-to-end distance in *trans*-azobenzene is known to be 9.0 Å,²⁷ rotation of half of the azobenzene requires a sphere of 4.5 Å in diameter. In addition, the critical volume required for the rearrangement is believed to contain some additional free volume provided by the matrix, which is difficult to estimate.²⁵ Therefore, a sphere of 4.5 Å may be the minimum size of free volume required for the isomerization, if photoisomerization takes place by the rotation mechanism. However, in view of the uncertainties involved, this value should be only viewed as a crude estimate.

Azo labels with smaller free volume in their vicinity cannot isomerize until free volume increases to such a critical size by a diffusion (redistribution) of free volumes. One plausible mechanism responsible for diffusion and coalescence of free volume is the main-chain segmental motion in the neighborhood of the label. Thus, the rate of merging of free volumes is the rate-determining step for those azo labels which originally have free volumes smaller than the critical size. With these assumptions, we may interpret α as related to the fraction of free volume above a certain critical size or to the amount of the high segmental mobility associated with less dense regions in solids. In regions of this high free volume, photoisomerization seems to occur without much difficulty, since A_1 is similar to the rate observed in dilute solution.

It is interesting to note that Robertson²⁸ in his molecular theory of physical aging based on rotation around short segments of the polymer main chain suggested that the initial fast volume relaxation is due to relaxing molecular rearrangements in regions of particularly high free volume produced by thermal fluctuations. He used a Γ distribution function of free volume sizes. As shown in Figure 6, α decreases as physical aging proceeds, reflecting the collapse of free volume larger than the critical size. This suggests that the free volume size distribution becomes skewed toward smaller sizes after aging. Similar conclusions have been reached by diffusion studies. For example, Levita and Smith^{15a} recently studied the dependence of the permeability and diffusion coefficient of several gases in glassy polymers on the extent of physical aging following a simple tensile deformation. The rates by which these transport coefficients decrease with aging time were found to be dependent on the size of the gas molecule; xenon exhibited a much faster decay rate than argon, which is smaller than xenon. They interpreted these results to mean that the larger size free volume (which would be required for xenon) collapses faster than the smaller size free volume (for argon) and the size distribution thus becomes skewed toward similar sizes as physical aging proceeds.

In assessing α , we used A_1 and A_2 values of 2×10^{-2} and $2 \times 10^{-4} \text{ s}^{-1}$, respectively, to fit the curves. The error in A_1 was relatively small ($\sim 15\%$), while in A_2 , it was greater, especially at lower temperatures. The reason for an increasing error in A_2 is due to the decrease in A_2 at lower temperatures. This trend is not unreasonable since A_2 must be related to the rate at which the free volume is redistributed. Such redistribution may occur by some segmental motion, which is a thermally activated process. It was of interest to determine the temperature dependence of A_2 . For this purpose, careful photochemical

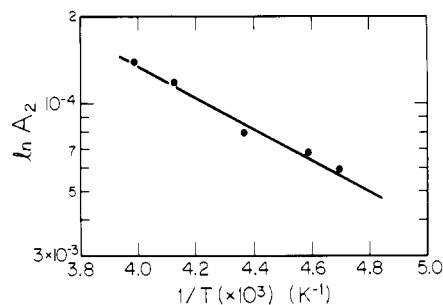


Figure 9. Arrhenius plot ($\ln A_2$ vs. $1/T$) to determine the activation energy for the slow photochemical rate process.

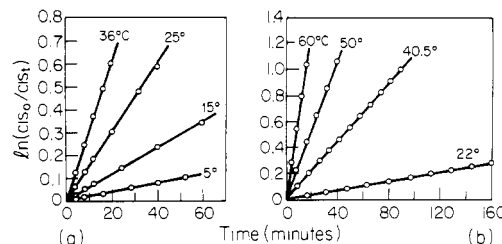


Figure 10. First-order plots of thermal $\text{cis} \rightarrow \text{trans}$ isomerization of azobenzene residues (a) in dilute solutions of pu-BD and (b) in the rubbery films of pu-PPO.

isomerization kinetics were carried out in the temperature range -60 to -20°C for quenched pu-PPO films. The A_2 values were obtained by extrapolating the linear regions (up to 400 s of irradiation time), and its temperature dependence is shown in Figure 9 as an Arrhenius plot. The activation energy from this plot is about 2.5 kcal/mol. Therefore, it appears that the process of the merging of the free volumes has an activation energy of 2.5 kcal/mol.

Within the range of A_2 values observed at the lower temperatures, however, the values of α are rather insensitive to A_2 . Thus, the error in α values when A_2 was assumed to be 2×10^{-4} were only about 10%.

It is important to point out that two distinct states of mobility in the glassy state have also been observed recently by other molecular probe/labeling studies. For example, in spin-probed and -labeled (in the side chain) poly(methyl methacrylate), Tsay et al.²⁹ observed that the ESR spectra were composed of narrow and broad components corresponding to fast and slow motions, respectively, even in the glassy state. They found that the fraction of the fast motion decreased with physical aging. They were able to interpret their results by also assuming that the spin label is either in a liquid-like state when the free volume is larger than the size of the label or in a solid-like state in case when the free volume is smaller. Thus it appears that two distinct states of mobility may be characteristic of the glassy state in general when probed by molecular labels.

(f) Thermal $\text{Cis} \rightarrow \text{Trans}$ Isomerization in Dilute Solution and in the Rubbery State. The thermal $\text{cis} \rightarrow \text{trans}$ isomerization of azo labels in the main chains of the polymers proceeds by first-order kinetics as long as they are in dilute solution or in a rubbery matrix. This is shown from the straight lines in the first-order plots ($\ln([cis]_0/[cis]_t)$ vs. time) in parts a and b of Figure 10, respectively. The rate constants (k_T) for thermal isomerization have been plotted as Arrhenius plots in Figure 11. We note the following trends from Figure 11: (a) The rate constants k_T vary within the same order of magnitude among three different polymers in dilute solutions. (b) In pu-PPO, the rate constants are slightly lower in the rubbery matrix than in dilute solution. In the rubbery matrix k_T is about half of its value in dilute solution. (c) The

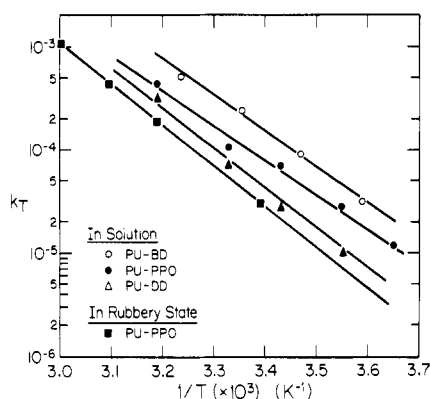


Figure 11. Arrhenius plots ($\ln k_T$ vs. $1/T$) of the thermal isomerization in dilute solutions and in the rubbery state.

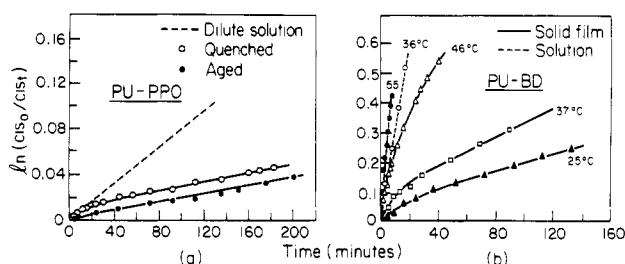


Figure 12. First-order plots of thermal cis \rightarrow trans isomerization of azobenzene residues for (a) pu-PPO at 3 °C (5 °C below T_g) and (b) pu-BD at indicated glassy and rubbery temperatures. Dotted lines in (a) and (b) correspond to dilute solution data.

activation energies, however, are quite similar as illustrated by similar slopes. For ΔE^* , values of 15–18 kcal/mol are obtained. This range of the activation energy has also been observed in dilute solutions of poly(methyl methacrylate) containing azo labels in its side chain.

(g) Thermal Cis \rightarrow Trans Isomerization in the Glassy State. While the thermal cis \rightarrow trans isomerization of azo labels in the main chain of our polymers follows strictly first-order kinetics in solution, it exhibits some deviation from first-order plots when studied in glassy matrices for all three polymers. An example is shown in Figure 12a for the pu-BD film covering rubbery and glassy matrices, in comparison to dilute solution (dotted line). We note from Figure 12a the linearity in the rubbery state (55 °C) and the deviation in the glassy states. The thermal isomerization is also slower in the glassy state than in dilute solution (compare the dotted line and a solid line at 37 °C). In these experiments, the glassy films were cast, dried, and annealed at the same temperature as the thermal isomerization temperature. Therefore, they should correspond to a well-aged sample, as indicated by their photoisomerization behavior.

In order to study the effect of physical aging on thermal isomerization, pu-PPO film was investigated at 5 °C below its T_g . Figure 12b shows the results. The dotted straight line corresponds to the first-order plot in dilute solution at 3 °C. Two curves correspond to the glassy-state reaction at the same temperature, before and after aging for 18 h, respectively. Aging for 18 h at 3 °C is expected to bring the glass near equilibrium. Subsequent to the photoisomerization in the rubbery state (around 27 °C), thermal isomerization was either followed immediately for the quenched state or after aging the sample for 18 h with continued irradiation of the sample.

From Figure 12b we note that the thermal isomerization in the glassy matrix is slower than in dilute solution. However, except for a very small deviation in the early state of the reaction, the reaction (as determined from the

Table II
Analyses of Thermal Cis \rightarrow Trans Isomerization of Azo Labels in the Main Chains of pu-PPO at 3 °C

state	K_a , s^{-1} ^a	$(1 - \beta)$ ^b
quenched glass	3.1×10^{-6}	0.987
aged glass ^c	2.8×10^{-6}	0.998
dilute solution	1.4×10^{-5}	1.000
extrapolated from rubbery state	3.7×10^{-6}	1.000

^a Rate constant for linear portion. ^b Fraction which proceeds by the rate constant K_a . ^c Aged for 18 h at 3 °C prior to thermal isomerization.

slope of the near-linear portion) proceeds with a rate similar to the extrapolated value from the rubbery state. The analyses of the two lower curves indicate that, as shown in Table II, only a very small fraction (β) deviates from the rest of the moieties. Except for this small deviation, the difficulty experienced for the thermal isomerization is similar for both the rubbery and glassy state. Table II shows also that the aging, at least at this temperature, has a rather small effect on the thermal isomerization since the changes in kinetic parameters are small. This tendency may not be so surprising since the time scale of thermal reaction is long enough to allow redistribution of free volume in the vicinity of the azo label. It appears from these results that due to the slower rate of thermal isomerization, it is difficult to obtain quantitative information on free volume and its size distribution by monitoring thermal isomerization. However, these results on thermal isomerization are useful in that they provide conclusive experimental evidence that conformational transitions even double bonds can occur in the glassy state, even though they are slower than in dilute solution.

Future Studies

It is obvious from the results of this study that the time scale of photoisomerization measurement is in the hundreds of seconds. During such time, free volume may be redistributed as well as decreased to some extent. In order to obtain information on the dynamics of the polymer system without such complications, it is desirable to carry out time-resolved spectroscopy following short (e.g., nanosecond) pulses of irradiation.

Preliminary studies using nanosecond pulses of a 353-nm beam from a Nd:YAG laser as an irradiating source indicate that photoisomerization occurs even in the solid films of pu-PPO as well as in dilute solution during a 2-ns flash.

It will also be interesting to label the polymer chain at specific sites and to follow physical aging by photoisomerization as a function of the location of the label in the chain.

We are planning to continue our future studies in these two directions.

Acknowledgment. We acknowledge financial support of this work in part by the National Science Foundation, Polymers Program (Grant No. DMR 78-07172), and the Whitaker Health Sciences Fund. We are grateful to Professors H. Morawetz, W. Stockmayer, E. W. Merrill, and R. Simha and Dr. Robertson for helpful discussions and encouragement and to Dr. P. Calvert and Professor N. H. Sung for critical reading of the manuscript. C.S.P.S. acknowledges the hospitality of Professor Turro's group during her stay to use flash photolysis equipment at Columbia University.

Registry No. Toluene 2,4-diisocyanate-4,4'-diaminoazobenzene-1,4-butanediol terpolymer, 87157-00-4; toluene 2,4-diisocyanate-4,4'-diaminoazobenzene-1,10-decanediol terpolymer,

87157-01-5; toluene 2,4-diisocyanate-4,4'-diaminoazobenzene-1,2-propanediol terpolymer, 87157-02-6.

References and Notes

- (1) For a recent collection of papers on physical aging, see *Polym. Eng. Sci.*, **21** (1981), and *Ann. N.Y. Acad. Sci.*, "Structure and Mobility in Molecular and Atomic Glasses", J. M. O'Reilly and M. Goldstein, Eds., 1981.
- (2) L. G. E. Struik, "Physical Aging in Amorphous Polymers and Other Materials", Elsevier, New York, 1978.
- (3) To list a few theoretical studies: (a) A. J. Kovacs, J. J. Aklonis, J. M. Hutchinson, and A. R. Ramos, *J. Polym. Sci., Polym. Phys. Ed.*, **17**, 1097 (1979); (b) R. E. Robertson, *ibid.*, **17**, 597 (1979).
- (4) (a) A. J. Kovacs, *Fortschr. Hochpolym.-Forsch.*, **3**, 394 (1963); (b) G. Goldbach and G. Rehage, *Rheol. Acta*, **6**, 30 (1967); *J. Polym. Sci., Part C*, **16**, 2289 (1967).
- (5) (a) S. E. B. Petrie, *J. Polym. Sci., Part A-2*, **10**, 1255 (1972); (b) R. Straff and D. R. Uhlmann, *J. Polym. Sci., Polym. Phys. Ed.*, **14**, 1087 (1976); (c) R. E. Robertson, *J. Appl. Phys.*, **49**, 5048 (1978).
- (6) S. E. B. Petrie, *J. Macromol. Sci., Phys.*, **B12** (2), 225 (1976).
- (7) J. L. R. Williams and R. C. Daly, *Prog. Polym. Sci.*, **5**, 61 (1977).
- (8) (a) Z. Veksli and W. G. Miller, *Macromolecules*, **10**, 686 (1977); (b) K. Murakami and J. Sohma, *Polym. J.*, **11**, 454 (1979).
- (9) K. Y. Law and R. O. Loutfy, *Macromolecules*, **14**, 587 (1981).
- (10) To list a few recent studies: (a) P. Bortolus and S. Monti, *J. Phys. Chem.*, **83**, 648 (1979); (b) H. Borner, H. Gruen, and D. J. Schulte-Frohlinde, *ibid.*, **84**, 3031 (1980); (c) H. Rau and E. Luddecke, *J. Am. Chem. Soc.*, **104**, 1616 (1982).
- (11) C. S. Paik and H. Morawetz, *Macromolecules*, **5**, 171 (1972).
- (12) C. D. Eisenbach, *Makromol. Chem.*, **179**, 2489 (1978).
- (13) D. T.-L. Chen and H. Morawetz, *Macromolecules*, **9**, 463 (1976).
- (14) (a) C. S. P. Sung, L. Lamarre, and K. H. Chung, *Macromolecules*, **14**, 1839 (1981); (b) L. Lamarre, Ph.D. Thesis, Department of Materials Science and Engineering, M.I.T., 1983.
- (15) (a) G. Levita and T. L. Smith, *Polym. Eng. Sci.*, **21**, 936 (1981); (b) S. Matsuoka, *ibid.*, **21**, 907 (1981).
- (16) (a) R. Simha, *Polym. Eng. Sci.*, **20**, 82 (1980); (b) I. G. Brown, R. E. Wetton, M. J. Richardson, and N. G. Savill, *Polymer*, **19**, 659 (1978).
- (17) T. Kajiyama and W. J. MacKnight, *Trans. Soc. Rheol.*, **13-14**, 527 (1969).
- (18) (a) G. Zimmerman, L.-Y. Chow, and U.-J. Paik, *J. Am. Chem. Soc.*, **80**, 3528 (1958); (b) J. Blanc, *J. Phys. Chem.*, **74**, 4037 (1970).
- (19) Without curve resolution, the kinetics plot is linear up to 75% conversion but, after that, shows some curvature due to the error in reading optical density accurately at higher conversion.
- (20) M. Irie and W. Schnabel, *Macromolecules*, **14**, 1246 (1981).
- (21) (a) A. W. Lawson, *J. Phys. Chem. Solids*, **3**, 250 (1957); (b) R. W. Keyes, *J. Chem. Phys.*, **29**, 467 (1958).
- (22) R. F. Boyer and P. L. Kumler, *Macromolecules*, **10**, 461 (1977).
- (23) (a) S. E. B. Petrie, *J. Polym. Sci., Part A-2*, **10**, 255 (1972); (b) R. Straff and D. R. Uhlmann, *J. Polym. Sci., Polym. Phys. Ed.*, **14**, 1087 (1976); (c) R. E. Robertson, *J. Appl. Phys.*, **49**, 5048 (1978).
- (24) T. L. Smith and R. E. Adam, *Polymer*, **22**, 299 (1981).
- (25) D. Gegiou, K. A. Muszkat, and E. Fischer, *J. Am. Chem. Soc.*, **90**, 12 (1968).
- (26) V. I. Pergushov, O. M. Mikhailik, A. Kh. Vorobev, and V. S. Gurman, *Khim. Vys. Energ.*, **12**, 53 (1978).
- (27) (a) J. J. deLange, J. M. Robertson, and I. Woodward, *Proc. R. Soc. London, Ser. A*, **171**, 398 (1939); (b) G. C. Hampson and J. M. Robertson, *J. Chem. Soc.*, 409 (1941).
- (28) R. E. Robertson, *J. Polym. Sci., Polym. Symp.*, **No. 63**, 173 (1978).
- (29) F. D. Tsay, S. D. Hong, J. Moacanin, and A. Gupta, *J. Polym. Sci., Polym. Phys. Ed.*, **20**, 763 (1982).

Mass Spectrometric Study of Interactions between Poly(ethylene glycols) and Alkali Metals in Solution

Kelvin W. S. Chan and Kelsey D. Cook*

School of Chemical Sciences and Materials Research Laboratory, University of Illinois, Urbana, Illinois 61801. Received January 24, 1983

ABSTRACT: Solution-phase ion-polymer interactions between poly(ethylene glycols) (PEG's) and alkali metal ions (in glycerol) were studied by electrohydrodynamic ionization mass spectrometry. Metal complexes of different oligomers (with degree of polymerization (n) as low as 4) were resolved. Mass spectral intensities of these complex ions supported the prediction of multiple-ion association by larger oligomers. The minimum n required for this multiple-ion association correlated positively with the size of the metal ion. In EH mass spectra of glycerol solutions containing PEG and more than one metal ion, preferential complexation by the PEG oligomers for one metal over another was observed. From the total spectral intensities of each metal complex, bulk selectivity of PEG for alkali metal ions was found to follow the order $K^+ > Cs^+ > Rb^+ > Na^+ > Li^+$ (1:0.94:0.79:0.46:0.08). These findings generally agreed with studies by other methods, although detection of lithium-PEG adducts has apparently not been previously reported in protic solvents.

Introduction

Interactions between metal ions and macromolecules play a fundamental role in many important phenomena, including selective transport of metal ions through membranes,¹ phase-transfer catalysis,² and biological enzyme systems.³ To understand these interactions, properties such as the stoichiometry and structure of complexes formed, the site(s) of interaction, and the binding ability and selectivity of a given polymer for various metals have to be characterized. This study considers a way of probing two of these (the binding ability and selectivity), using a poly(ethylene glycol) model system in glycerol.

Linear poly(ethylene glycols) $(HO-(CH_2CH_2O)_n-H)$, PEG's) of low molecular weight predominantly exist in a "zigzag" form, resulting in an open-coil extended conformation.⁴ Chains longer than nine repeat units prefer the

"meander" conformation, giving a more compact helical coil.⁴ These chains form complexes with a variety of metals. The interactions between the polymer and metal ions are believed to involve the same kind of ion-dipole interactions observed in cyclic polyethers. In fact, proton,⁵⁻⁷ carbon-13,^{5,8} and sodium-23⁹⁻¹¹ magnetic resonance experiments have confirmed that the ethereal oxygens on the oxyethylene units of both PEG's and crown ethers are the sites of interaction with metal ions. Despite the similarity in their interaction mechanism, the complexing ability of noncyclic polyethers can differ markedly from that of their cyclic analogues. Yanagida et al.,¹² using a solvent extraction method, reported that the extracting ability of PEG is related to the number of repeating units on the chain. The extracting ability of low molecular weight PEG's ($n < 40$) for K^+ was smaller than that of